Research Paper
Computational Methods for Differential Equations
http://cmde.tabrizu.ac.ir
Vol. *, No. *, *, pp. 1-14
DOI:10.22034/cmde.2026.73225.3725

A non-dyadic higher order Haar wavelet collocation technique for one dimensional Gelfand problem

Ritesh Gupta[1], Mandeep Singh[1,*], and Salman Raju Talluri[2]

[1]Department of Mathematics, JUIT, Waknaghat, Solan, HP, India.

[2]Department of Electronics and Communication Engineering , JUIT, Waknaghat, Solan, HP, India.

Abstract

This study investigates the numerical solution of one dimensional Gelfand's problem, widely known as Bratu's problem, using both the non-dyadic Haar wavelet and its higher order Haar wavelet collocation technique. A comprehensive comparison of the numerical results obtained using these methods is presented to evaluate their accuracy and effectiveness. Using the Haar wavelet operational matrix, the highly non-linear differential equation reduces to a system of non-linear algebraic equations that can be further solved efficiently with Newton-Raphson technique. The accuracy and convergence of the proposed method are examined using the maximum absolute error, l_2-norm error and rate of convergence and compared with existing numerical techniques. Numerical findings show that non-dyadic higher order Haar wavelet method provides the better precision and high rate of convergence than the classical non-dyadic Haar wavelet approach, although both techniques agree closely with available solutions.

Keywords. Higher order Haar wavelet method; Collocation points; Non-dyadic; Bratu's problem; Newton-Raphson method.

2010 Mathematics Subject Classification. 34B15, 65L10, 65T60.

Uncorrected

1. Introduction

The Gelfand problem, which models thermal explosions using a non-linear elliptic equation is provided by

$$\begin{cases} \Delta u + \lambda e^{\alpha u} = 0, & \text{in} \quad \Omega, \\ u = 0, & \text{on} \quad \partial\Omega, \end{cases} \tag{1.1}$$

where λ, α are physical parameters and $\Omega = \{x \in \mathbb{R}^m : \|x\| \leq 1\}$ is a bounded domain. It is initially investigated by D.A. Frank-Kamenetskii [15, 36] in 1938 and subsequently popularized by Gelfand[17]. The same kind of problems (with different dimensional variants [43]) have been actively explored because of its complex mathematical structure and great physical importance [16].The solution structure depends strongly on the dimension: in low dimensions ($m \leq 2$) there exists a critical value λ_c such that solutions exist only for $\lambda \leq \lambda_c$, whereas in higher dimensions the solution branches become oscillatory [20].

The one-dimensional reduction of this elliptic problem leads to the Bratu-type ordinary differential equation considered in the present study. Throughout this paper, the term Bratu's problem refers specifically to the one-dimensional boundary value problem is given by

$$y''(x) + \lambda e^{\alpha y(x)} = 0; \quad 0 \leq x \leq 1, \tag{1.2}$$

$$y(0) = 0, \quad y(1) = 0, \tag{1.3}$$

where λ is a real constant and α is constant taken as $\alpha = \pm 1$. Bratu's problems is initially formulated to elucidate thermal ignition, has been extended to various physical domains, including chemical reactor theory, combustion, and astrophysics, highlighting its extensive applicability and theoretical importance.

Received: 24 June 2026; Accepted: 15 November 2026.
∗ Corresponding author. Email: mandeep04may@yahoo.in.

The exact closed form solution for the considered problem (1.2)-(1.3), corresponding to $\alpha = 1$ and $\lambda > 0$, has been analysed by [6, 7], where the analytical structure and characteristics are thoroughly investigated and is

$$y(x) = -2\log\left[\frac{\cosh\left(\left(x-\frac{1}{2}\right)\frac{\theta}{2}\right)}{\cosh\left(\frac{\theta}{2}\right)}\right], \tag{1.4}$$

where the parameter θ is determined implicitly from the transcendental equation

$$\theta = \sqrt{2\lambda}\cosh\left(\frac{\theta}{4}\right). \tag{1.5}$$

The solution behavior of Bratu's problem is controlled by the parameter λ with a critical turning point λ_c. The problem admits no solution for $\lambda > \lambda_c$, a unique solution for $\lambda = \lambda_c$, and two distinct solutions for $\lambda < \lambda_c$. This critical point λ_c satisfies the condition

$$1 = \frac{1}{4}\sqrt{2\lambda_c}\sinh\left(\frac{\theta_c}{4}\right), \tag{1.6}$$

and $\lambda_c \approx 3.513830719$ can be evaluated numerically using e.g., Newton's method or MATLAB in-built function fzero for root-finding problems.

Due to the scientific significance of Bratu's problem, over the past decades, various types of numerical and analytical techniques have been developed to obtain accurate and efficient solutions, such as Adomian decomposition [42], Laplace transform decomposition method (LTDM) [23], robust Lucas-Fibonacci series approach [14], generalized bessel quasilinearization method [19], iterative finite difference techniques in conjunction with Newton–Raphson–Kantorovich that effectively manage exponential non-linearity[**?**], finite difference spectral collocation schemes with quasilinearization, Chebyshev polynomials, and Sumudu transforms for high-accuracy one-dimensional solutions[3], spectral and pseudospectral techniques, particularly those based on Chebyshev polynomials [9]. A bio-inspired neural network model [34] optimized via a genetic algorithm for the development of the efficiently solved Bratu's type equation, which governs electrically conducting solids.

In this study, the non-dyadic (especially scale-3) Haar wavelet collocation method (HWCM-S3) and its advancement, i.e., higher order Haar wavelet collocation method (HOHWCM-S3), are developed and employed for the numerical investigation of the Bratu's problem. The higher order Haar wavelet collocation method (HOHWCM) is an enhanced version of the classic Haar wavelet method that improves the numerical accuracy. Due to higher order expansions within each subinterval, it overcomes the low-order convergence of piecewise-constant Haar bases. This leads to high rate of convergence than the classical non-dyadic Haar wavelet and increased accuracy for smooth solutions, while preserving the simplicity and sparsity of the Haar framework. Researchers [24, 39, 41] methodically developed HOHWCM (for the dyadic case) for different kinds of non-linear boundary value problems. In this study, we establish the higher order Haar wavelet concept for scale-3.

The present research paper is organized in four sections: Section 2 provides the fundamental notion of the scale-3 Haar wavelet basis and their integrals. This section also consist of the implementation of HWCM-S3 and its advancement (HOHWCM-S3) on Bratu's problem. Section 3 provides numerical illustrations of Bratu's problem for different values of parameter λ. Numerical findings are also compared with existing methods to describe the efficiency as well as effectiveness of suggested method. Results and conclusions drawn from the tested problems are compiled in the final section.

Uncorrected Proof

2. Non-dyadic Haar wavelet: Scale-3

The classical Haar wavelet was the first wavelet introduced by Alfred Haar in 1910. It is defined on successively halved intervals (dyadic partitions), which means that the scale of the wavelet functions varies by powers of two. This structure generates an orthonormal wavelet basis and allows for rapid wavelet transforms, making Haar wavelets popular for signal decomposition and numerical analysis. For an exhaustive review of Haar wavelet theory and its applications (including dyadic constructs), see references [4, 21, 25, 33, 37]. In contrast to traditional dyadic or scale-2 construction, scale-3 or non-dyadic Haar wavelets use partitions based on three scales (or other non-power-of-two nodals) rather than the usual dyadic (power-of-two) approach. This generalisation frequently uses more than one

mother wavelet function to generate the wavelet family, like the scale-3 Haar wavelet, which is generated from two basic mother wavelets, one symmetric and the other non-symmetric. In recent literature, scale-3 Haar wavelets have been successfully employed for solving different kinds of differential equations with suitable conditions (for more details, see [5, 32]).

In scale-3, the scaling function satisfies the translation and dilation relation, which is defined as

$$\phi(x) = \sum_{i=0}^{M} a_i \phi(3x - i), \quad a_0, a_1, ..., a_M \neq 0. \tag{2.1}$$

Consider the subspace

$$U_j = \{\phi_{j,k}(x) = 3^{j/2}\phi(3^j x - k) : k \in \mathbb{Z}\}, \quad V_j = \overline{U_j}, \quad j \in \mathbb{Z}. \tag{2.2}$$

The family $\{\phi_{j,k}(x)\}$ form a complete orthonormal basis of V_j. The nested sequence of subspace $V_j \subset V_{j+1}$ at different level j, whose union is dense in the space $L^2(\mathbb{R})$ constitutes a multiresolution analysis. The core idea of multiresolution analysis is the decomposition of the function into components for describing its behavior across multiple resolutions. For each j, let W_j be the orthogonal complement of V_j in V_{j+1}. Therefore, W_j and V_j are subspace of V_{j+1}. If W_j is spanned by non-dyadic (scale-3) Haar wavelet basis function $\{h_{j,k} : j, k\epsilon\mathbb{Z}\}$, using the classical construction of Chui and Lain [11], two compactly supported orthogonal functions $\psi(x)$, $\varphi(x)$ ϵ $W_0 \subset V_1$ have occurred. The non-dyadic (scale-3) Haar scaling function $h_1(x)$, symmetric function $\psi(x)$, and anti-symmetric function $\varphi(x)$ are in pictorial and function form in [29].

To define the general formula for Haar wavelet family on scale-3, we use the concepts of scaling, symmetric & anti-symmetric, and also divide the integration domain $[0, 1]$ into $3M$ equal sub-intervals each with length $\Delta(x) = \frac{1}{3M}$. The formula $i = m + 2\gamma + 1$(symmetric wavelet) and $i = m + 2\gamma + 3$ (anti-symmetric wavelet) yields the parameter i. Define $M = 3^J$ and let J be the maximum degree of resolution. The uniform Haar wavelets is defined as

$$h_1(x) = \begin{cases} 1, & x \in [0, 1), \\ 0, & elsewhere, \end{cases} \tag{2.3}$$

for symmetric Haar wavelet $(i = 2, 4, 6, ..., 3M - 1)$,

$$\psi_i(x) = \frac{1}{\sqrt{2}} \begin{cases} 1, & x \in [\alpha_1(i), \alpha_2(i)), \\ 2, & x \in [\alpha_2(i), \alpha_3(i)), \\ -1, & x \in [\alpha_3(i), \alpha_4(i)), \\ 0, & elsewhere, \end{cases} \tag{2.4}$$

for anti-symmetric Haar wavelet $(i = 3, 5, 7, ..., 3M)$,

$$\varphi_i(x) = \sqrt{\frac{3}{2}} \begin{cases} 1, & x \in [\alpha_1(i), \alpha_2(i)), \\ 0, & x \in [\alpha_2(i), \alpha_3(i)), \\ -1, & x \in [\alpha_3(i), \alpha_4(i)), \\ 0, & elsewhere, \end{cases} \tag{2.5}$$

where

$$\begin{cases} \alpha_1(i) = \dfrac{\gamma}{m}, \\ \alpha_2(i) = \dfrac{(\gamma + \frac{1}{3})}{m}, \\ \alpha_3(i) = \dfrac{(\gamma + \frac{2}{3})}{m}, \\ \alpha_4(i) = \dfrac{(\gamma + 1)}{m}, \end{cases} \tag{2.6}$$

Uncorrected Proof

where $m = 3^j$, $j = 0, 1, 2, ..., J$, $\gamma = 0, 1, 2, ..., m-1$. A closed form analytical expression for the general integral (i.e., n^{th} order) of the Haar functions can be obtained as

$$Q_{n,i}(x) = \sqrt{\frac{1}{2}} \begin{cases} 0, & x \in [0, \alpha_1(i)), \\ \frac{-1}{n!}[x - \alpha_1(i)]^n, & x \in [\alpha_1(i), \alpha_2(i)), \\ \frac{1}{n!}\left[-(x-\alpha_1(i))^n + 3(x-\alpha_2(i))^n\right], & x \in [\alpha_2(i), \alpha_3(i)), \\ \frac{1}{n!}\left[-(x-\alpha_1(i))^n + 3(x-\alpha_2(i))^n - 3(x-\alpha_3(i))^n\right], & x \in [\alpha_3(i), \alpha_4(i)), \\ \frac{1}{n!}\left[-(x-\alpha_1(i))^n + 3(x-\alpha_2(i))^n - 3(x-\alpha_3(i))^n + (x-\alpha_4(i))^n\right], & x \in [\alpha_4(i), 1), \end{cases} \tag{2.7}$$

where $Q_{n,i}(x)'s$ are even wavelet, i.e. $i = 2, 4, 6, ..., 3M-1$.

For odd wavelet $R_{n,i}(x)'s$ i.e when $i = 3, 5, 7, ..., 3M$ is given by

$$R_{n,i}(x) = \sqrt{\frac{3}{2}} \begin{cases} 0, & x \in [0, \alpha_1(i)), \\ \frac{1}{n!}[x - \alpha_1(i)]^n, & x \in [\alpha_1(i), \alpha_2(i)), \\ \frac{1}{n!}\left[(x-\alpha_1(i))^n - (x-\alpha_2(i))^n\right], & x \in [\alpha_2(i), \alpha_3(i)), \\ \frac{1}{n!}\left[(x-\alpha_1(i))^n - (x-\alpha_2(i))^n - (x-\alpha_3(i))^n\right], & x \in [\alpha_3(i), \alpha_4(i)), \\ \frac{1}{n!}\left[(x-\alpha_1(i))^n - (x-\alpha_2(i))^n - (x-\alpha_3(i))^n + (x-\alpha_4(i))^n\right], & x \in [\alpha_4(i), 1), \end{cases} \tag{2.8}$$

and for $i = 1$, $P_{n,1}(x)$ is defined as

$$P_{n,1}(x) = \frac{x^n}{n!}. \tag{2.9}$$

To employ discrete Haar wavelets, the nodal points are provided by

$$\tilde{z}_\ell = \ell \Delta x, \quad \forall\, \ell = 0, 1, ..., 3M, \tag{2.10}$$

and collocation points are

$$x_\ell = \frac{\tilde{z}_{\ell-1} + \tilde{z}_\ell}{2}, \quad \forall\, \ell = 1, 2, ..., 3M. \tag{2.11}$$

2.1. **Formulation of HWCM-S3 and HOHWCM-S3.** In this section, we address the general description of HWCM-S3 and HOHWCM-S3 to obtain their corresponding solutions. Assume the n^{th} order differential equation

$$\phi\left(x, y, \frac{dy}{dx}, \frac{d^2y}{dx^2}, ..., \frac{d^ny}{dx^n}\right) = 0. \tag{2.12}$$

The highest-order derivative is expressed by Haar wavelets series expansion (for more details [29, 30])

$$\frac{d^ny}{dx^n} = a_1 h_1(x) + \sum_{\substack{i\geq 2, \\ i=even}}^{3M-1} a_i \psi_i(x) + \sum_{\substack{i\geq 3, \\ i=odd}}^{3M} a_i \varphi_i(x), \tag{2.13}$$

where a_i's are the wavelet coefficients. The solution $y(x)$ of the differential equation (2.12) is derived by performing successive integrations of Eq. (2.13) repeated n times

$$y(x) = a_1 P_{n,1}(x) + \sum_{\substack{i\geq 2, \\ i=even}}^{3M-1} a_i Q_{n,i}(x) + \sum_{\substack{i\geq 3, \\ i=odd}}^{3M} a_i R_{n,i}(x) + \sum_{r=0}^{n-1} b_r \frac{x^r}{r!}, \tag{2.14}$$

where b_r's are the arbitrary constants, and can be determined by the given boundary conditions. This approaches is generally known as the classical non-dyadic (scale-3) Haar wavelet collocation method (HWCM-S3).

To improve the accuracy, we use the advancement of HWCM-S3 i.e., higher order Haar wavelet collocation method (HOHWCM-S3). In this approach, the Haar wavelet series expansion is written as

Uncorrected Proof

$$\frac{d^{n+2\mu}y}{dx^{n+2\mu}} = a_1 h_1(x) + \sum_{\substack{i\geq 2,\\ i=even}}^{3M-1} a_i \psi_i(x) + \sum_{\substack{i\geq 3,\\ i=odd}}^{3M} a_i \varphi_i(x), \tag{2.15}$$

where $\mu = 1, 2, 3$ and so on (when $\mu = 0$, we arrive at the classical non-dyadic HWCM-S3). Integrating the Eq. (2.15) $n + 2\mu$ times, the approximate solution of differential equation is followed as

$$y(x) = a_1 P_{n+2\mu,1}(x) + \sum_{\substack{i\geq 2,\\ i=even}}^{3M-1} a_i Q_{n+2\mu,i}(x) + \sum_{\substack{i\geq 3,\\ i=odd}}^{3M} a_i R_{n+2\mu,i}(x) + c_1(x) + c_2(x), \tag{2.16}$$

where

$$c_1(x) = \sum_{r=0}^{n-1} b_r \frac{x^r}{r!} \quad and \quad c_2(x) = \sum_{r=n}^{n+2\mu-1} b_r \frac{x^r}{r!}.$$

In the above expression $c_1(x)$ and $c_2(x)$ collectively account for $n + 2\mu$ integration constants. The first n arbitrary constants can be find out from the given boundary conditions while remaining 2μ constants are obtained from the given differential equation at the uniform grid points located closest to the end points of the domain, i.e.,

$$\begin{cases} \phi\left(x_i, y, \frac{dy(x_i)}{dx}, \frac{d^2y(x_i)}{dx^2}, ..., \frac{d^n y(x_i)}{dx^n}\right) = 0, \\ x_i = \frac{i}{3M}, \quad x_i = 1 - \frac{i}{3M}, \qquad\qquad i = 0, 1, ..., \mu - 1. \end{cases} \tag{2.17}$$

Since this research is confined to the study of $\mu = 1$ only. The remaining two constants can be computed at the end points of the domain that satisfy the considered problem (2.12), i.e.,

$$\begin{cases} \phi\left(0, y(0), \frac{dy(0)}{dx}, \frac{d^2y(0)}{dx^2}, ..., \frac{d^n y(0)}{dx^n}\right) = 0, \\ \phi\left(1, y(1), \frac{dy(1)}{dx}, \frac{d^2y(1)}{dx^2}, ..., \frac{d^n y(1)}{dx^n}\right) = 0. \end{cases} \tag{2.18}$$

The more detailed explanation can be found in [26, 27].

2.2. **HWCM-S3 and HOHWCM-S3: Bratu's problem.** In this section, the non-linear Bratu's problem is solved by using HWCM-S3 and its advancement HOHWCM-S3, integrated with Newton-Raphson method. The defined boundary conditions are precisely incorporated into the wavelet formulation, yielding a system of non-linear algebraic equations that must be solved iteratively to get a convergent, stable, and accurate numerical solution. Based on the scale-3 Haar wavelet and higher order Haar wavelet, we can divide the algorithm in two categories, $\mu = 0$ and $\mu = 1$.

2.2.1. *HWCM-S3: Bratu's Problem.* For $n = 2$ and $\mu = 0$, Eq. (2.15) is equivalent to Eq. (2.13) and it is written as

$$\frac{d^2y}{dx^2} = a_1 h_1(x) + \sum_{\substack{i\geq 2,\\ i=even}}^{3M-1} a_i \psi_i(x) + \sum_{\substack{i\geq 3,\\ i=odd}}^{3M} a_i \varphi_i(x). \tag{2.19}$$

After integrating Eq. (2.19) two times successively, we get

$$y'(x) = a_1 P_{1,1}(x) + \sum_{\substack{i\geq 2,\\ i=even}}^{3M-1} a_i Q_{1,i}(x) + \sum_{\substack{i\geq 3,\\ i=odd}}^{3M} a_i R_{1,i}(x) + y'(0), \tag{2.20}$$

$$y(x) = a_1 P_{2,1}(x) + \sum_{\substack{i\geq 2,\\ i=even}}^{3M-1} a_i Q_{2,i}(x) + \sum_{\substack{i\geq 3,\\ i=odd}}^{3M} a_i R_{2,i}(x) + y'(0)x + y(0). \tag{2.21}$$

Uncorrected Proof

Now the boundary conditions given in Eq. (1.3) are imposed on Eq. (2.21) and resulting expression are substitute back to Eq. (1.2). One can obtain a system of nonlinear equations by substituting the collocation points for $x = x_l$.

$$\Xi_l(a_1, a_2, ..., a_{3M}) \equiv y''(x_l) + \lambda e^{\alpha y(x_l)} = 0, \quad \ell = 0, 1, ...3M, \tag{2.22}$$

where the quantities $y''(x)$ and $y(x)$ must be replaced according to the set of Eqs. (2.19) to (2.21). The unknown Haar wavelet coefficient $a_i's$ are determined by using the Newton–Raphson method. As per Newton-Raphson algorithm the r^{th} iteration is provided by

$$\sum_{i=1}^{3M} \left(\frac{\partial \Xi_l}{\partial a_i}\right)^r \Delta(a_i)^r = -\Xi_l^r, \tag{2.23}$$

where $\Delta(a_i)^r = a_i^{r+1} - a_i^r$. We can also write in the matrix form as

$$T^r \Delta(a)^r = -\Xi^r, \tag{2.24}$$

where $T = \frac{\partial \Xi_l}{\partial a_i}$ and $a = a_i$. This provide that

$$\Delta(a)^r = \left(-\Xi/T\right)^r. \tag{2.25}$$

The refined values for the Haar wavelet coefficient a can be calculated as

$$a^{r+1} = a^r + \Delta(a)^r. \tag{2.26}$$

The Haar wavelet coefficients a_i, $i = 1, 2, ..., 3M = 3^{J+1}$ are evaluated from Eq. (2.25). These coefficients are substituted into the wavelet expansion to yield the relevant approximate solution. To evaluated the wavelet coefficients on the subsequent resolution $J+1$, where the number of collocation points get triple. At this resolution we construct the initial guess, from the solution obtained at resolution J, by using the following approach

$$a_i{}^{J+1} = \begin{cases} a_i^J, & \text{if } i = 1, 2, ..., M, \\ 0, & \text{if } i = M+1, M+2, ..., 3M, \end{cases} \tag{2.27}$$

where a_i^J are wavelet coefficients which are preserved for resolution J. For $J = 0$, the initial guess is constructed using the prescribed boundary conditions.

2.2.2. *HOHWCM-S3: Bratu's Problem.* For $n = 2$ and $\mu = 1$, Eq. (2.15) becomes

$$\frac{d^4y}{dx^4} = a_1 h_1(x) + \sum_{\substack{i\geq 2,\\ i=even}}^{3M-1} a_i \psi_i(x) + \sum_{\substack{i\geq 3,\\ i=odd}}^{3M} a_i \varphi_i(x). \tag{2.28}$$

Integrate the Eq. (2.28) four times successively, we get

$$y'''(x) = a_1 P_{1,1}(x) + \sum_{\substack{i\geq 2,\\ i=even}}^{3M-1} a_i Q_{1,i}(x) + \sum_{\substack{i\geq 3,\\ i=odd}}^{3M} a_i R_{1,i}(x) + y'''(0), \tag{2.29}$$

$$y''(x) = a_1 P_{2,1}(x) + \sum_{\substack{i\geq 2,\\ i=even}}^{3M-1} a_i Q_{2,i}(x) + \sum_{\substack{i\geq 3,\\ i=odd}}^{3M} a_i R_{2,i}(x) + y'''(0)x + y''(0), \tag{2.30}$$

$$y'(x) = a_1 P_{3,1}(x) + \sum_{\substack{i\geq 2,\\ i=even}}^{3M-1} a_i Q_{3,i}(x) + \sum_{\substack{i\geq 3,\\ i=odd}}^{3M} a_i R_{3,i}(x) + y'''(0)\frac{x^2}{2!} + y''(0)x + y'(0), \tag{2.31}$$

$$y(x) = a_1 P_{4,1}(x) + \sum_{\substack{i\geq 2,\\ i=even}}^{3M-1} a_i Q_{4,i}(x) + \sum_{\substack{i\geq 3,\\ i=odd}}^{3M} a_i R_{4,i}(x) + y'''(0)\frac{x^3}{3!} + y''(0)\frac{x^2}{2!} + y'(0)x + y(0). \tag{2.32}$$

Uncorrected Proof

Making use the boundary condition (1.3), Eq. (2.32) becomes

$$y'(0) = -\left(a_1 P_{4,1}(1) + \sum_{\substack{i\geq 2,\\ i=even}}^{3M-1} a_i Q_{4,i}(1) + \sum_{\substack{i\geq 3,\\ i=odd}}^{3M} a_i R_{4,i}(1) + \frac{y'''(0)}{3!} + \frac{y''(0)}{2!} \right). \tag{2.33}$$

Next, with the help of B.C. (1.3) and the condition obtained by substituting the end points of the domain in problem (1.2), we obtain the following condition to obtain the additional 2μ constraints (see Eq. (2.18)),

$$\phi\left(0, y(0), y'(0), y''(0)\right) \equiv y''(0) + \lambda e^{\alpha y(0)} = 0 \implies y''(0) = -\lambda, \tag{2.34}$$

$$\phi\left(1, y(1), y'(1), y''(1)\right) \equiv y''(1) + \lambda e^{\alpha y(1)} = 0 \implies y''(1) = -\lambda. \tag{2.35}$$

At $x = 1$, applying the additional condition (2.35), in Eq. (2.30) we get

$$y'''(0) = -\left(a_1 P_{2,1}(1) + \sum_{\substack{i\geq 2,\\ i=even}}^{3M-1} a_i Q_{2,i}(1) + \sum_{\substack{i\geq 3,\\ i=odd}}^{3M} a_i R_{2,i}(1) \right). \tag{2.36}$$

With the help of Eqs. (1.3), (2.33), (2.34) and (2.36), the Eq. (2.32) becomes

$$\begin{aligned} y(x) = a_1 \left[(P_{4,1}(x) - P_{4,1}(1)x) + \frac{P_{2,1}(1)}{3!}(x - x^3) \right] + \sum_{\substack{i\geq 2,\\ i=even}}^{3M-1} a_i \left[(Q_{4,i}(x) - Q_{4,i}(1)x) + \frac{Q_{2,i}(1)}{3!}(x - x^3) \right] \\ + \sum_{\substack{i\geq 3,\\ i=odd}}^{3M} a_i \left[(R_{4,i}(x) - R_{4,i}(1)x) + \frac{R_{2,i}(1)}{3!}(x - x^3) \right] + \frac{\lambda}{2!}(x - x^2). \end{aligned} \tag{2.37}$$

Using the same process as in Section 2.2.1, we apply the Newton-Raphson method to obtain consecutive approximations that converge to the roots of the aforementioned equation.

Algorithm 1 Adaptive Haar Wavelet Method and Its Advancement for Bratu's Problem

1: Initialize the resolution level as $J = 0$.
2: Construct the nodal and collocation points corresponding to the current resolution level, as given in Eqs. (2.10) and (2.11).
3: For this problem ($n = 2$), the HWCM-S3 approximates $y''(x)$, whereas the HOHWCM-S3 approximates $y^{(n+2\mu)}(x)$, which for $\mu = 1$ is $y^4(x)$. The corresponding Haar wavelet expansions are given in Eq. (2.19) and Eq. (2.28), respectively.
4: Integrate the corresponding expansion successively to obtain the required lower-order derivatives and the approximate solution.
5: Determine the integration constants: the n constants of the HWM from the prescribed conditions in Eq. (1.3), and the $n + 2\mu$ constants of the HOHWCM-S3 ($n = 2$, $\mu = 1$) from these together with the additional conditions in Eqs. (2.34) and (2.35).
6: Substitute the resulting approximations into Bratu's equation (1.2) and impose the equation at the collocation points to obtain a nonlinear algebraic system in the unknown Haar wavelet coefficients a_i.
7: Solve the resulting nonlinear algebraic system for the Haar wavelet coefficients using the Newton–Raphson method.
8: Compute the numerical solution and evaluate the errors by comparing the numerical solution with the exact solution.
9: If the desired accuracy is achieved, stop. Otherwise, increase the resolution level from J to $J + 1$, update the Haar wavelet coefficients according to the initial-guess procedure described in Eq. (2.27), and repeat the above steps.

3. Numerical illustration

To illustrate the reliability, performance, and numerical robustness of the proposed enhancement of the non-dyadic (scale-3) Haar wavelet collocation method, referred to as the higher order Haar wavelet collocation method, one-dimensional non-linear Bratu-type problems are examined. To compare numerical findings with existing literature, cubic spline interpolation is employed to evaluate the numerical solution at arbitrary nodal points. Furthermore,

Uncorrected Proof

the rate of convergence is also determined, which confirms the proposed HOHWCM-S3 accuracy and efficiency. The accuracy of the numerical findings is evaluated using different error measures such as absolute error[3.1,1], l_2-norm error[3.2], maximum absolute error[3.3] and rate of convergence[3.4]. All computations are carried out using MATLAB R2019a on an HP laptop equipped with a 13^{th} Gen Intel® Core™ i7-13620H processor operating at 2.40 GHz.

Definition 3.1 (Absolute Error)**.** The absolute error at a point x is defined as the non-negative magnitude of the difference between the exact solution $\bar{y}(x)$ and the corresponding approximate solution $y(x)$, and is given by

$$E_{\text{abs}}(x) = |\bar{y}(x) - y(x)|\,.$$

Definition 3.2 (l_2-Norm Error)**.** It provides a measure of the deviation of the approximate solution from the exact solution over [0,1] and is defined as

$$E_{l_2} = \left(\Delta x \sum |\bar{y}(x) - y(x)|^2\right)^{1/2}.$$

Definition 3.3 (Maximum Absolute Error)**.** It is defined as the largest pointwise difference between the exact solution and the approximate solution over all collocation points and is expressed as

$$e_J = \max |\bar{y}(x) - y(x)|\,.$$

Definition 3.4 (Rate of Convergence [8, 31])**.** It measures the speed at which the numerical solution approaches the exact solution as the nodal is refined and is defined by

$$\text{ROC} = \frac{1}{\log 3} \log\left(\frac{e_{J-1}}{e_J}\right).$$

Example 3.1. *Consider a Bratu's problem*

$$y'' + \lambda e^y = 0; \quad \lambda < \lambda_c, \quad 0 \le x \le 1, \tag{3.1}$$

$$y(0) = y(1) = 0. \tag{3.2}$$

Here, we consider the Bratu's problem, when the parameter λ belongs to rational numbers. For comparison purpose, we discuss this problem for $\lambda = 0.5, 1, 2, 3$. The numerical results presented in tables 1 to 4 demonstrate the performance of HWCM-S3 and HOHWCM-S3 in terms of maximum absolute error, l_2-norm error, rate of convergence and CPU time (in sec). It is observed that, for both methods, the maximum absolute error and the l_2-norm error decrease monotonically as the resolution increases, indicating improved accuracy with mesh refinement.

Furthermore, HOHWCM-S3 achieves a ROC of nearly 4, which is higher than HWCM-S3, Iterative finite difference (IFD) [40], cubic B-spline [2] (all of which converge at a rate of nearly 2). This ROC is equivalent to optimal B-spline method [2], dyadic higher order Haar wavelet collocation method [38], and QBSM [35], which also contain fourth-order convergence. But, due to ease of implementation, HOHWCM-S3 achieved better accuracy in comparison to these methods.

Tables 5 and 6 present a comparative analysis of the absolute errors obtained using HOHWCM-S3 and several existing numerical techniques, HOHWCM-S2 [38], with $J = 9$; Lie-group shooting method (LGSM) [1], adopting a step size of $h = 0.0001$; differential transformation method (DTM) [18], LTDM [23], employing four iterations; B-spline [10], utilizing $n = 61$ mesh points; Iterative finite difference (IFD) [40], implementing with the mesh size of $M = 1000$; Decomposition [12], in which the infinite series is truncated after four terms. Figures 1 and 2 demonstrates that the proposed method gives a better results than the other existing methods.

[3.1,3.2,3.3,3.4] refers as Definition 3.1,3.2,3.3, and 3.4 respectively.

Uncorrected Proof

TABLE 1. Maximum absolute error of HWCM and HOHWCM solution on scale-3 for $\lambda = 0.5$ at different resolutions (J) together with the corresponding rate of convergence (ROC) and l_2-norm error (E_{l_2}) for Example 3.1.

J	HWCM-S3				HOHWCM-S3			
	e_J	E_{l_2}	ROC	CPU (in sec.)	e_J	E_{l_2}	ROC	CPU (in sec.)
0	1.40555E-04	9.77298E-05	–	0.11	3.38895E-06	2.39280E-06	–	0.16
1	1.82498E-05	3.95355E-05	1.86	0.15	4.08987E-08	8.82980E-08	4.02	0.14
2	2.06007E-06	1.34318E-05	1.99	0.28	5.03916E-10	3.26421E-09	4.00	0.22
3	2.29296E-07	4.48665E-06	2.00	0.35	6.22001E-12	1.20874E-10	4.00	0.47
4	2.54822E-08	1.49590E-06	2.00	1.39	7.71189E-14	4.48652E-12	4.00	2.51
5	2.83142E-09	4.98645E-07	2.00	10.0	1.38778E-15	2.00638E-13	3.66	11.62

TABLE 2. Maximum absolute error of HWCM and HOHWCM solution on scale-3 for $\lambda = 1$ at different resolutions (J) together with the corresponding rate of convergence (ROC) and l_2-norm error (E_{l_2}) for Example 3.1.

J	HWCM-S3				HOHWCM-S3			
	e_J	E_{l_2}	ROC	CPU (in sec.)	e_J	E_{l_2}	ROC	CPU (in sec.)
0	6.70396E-04	4.68532E-04	–	0.13	3.28946E-05	2.32489E-05	–	0.32
1	8.63674E-05	1.85810E-04	1.87	0.16	3.95025E-07	8.39792E-07	4.02	0.09
2	9.74192E-06	6.30147E-05	1.99	0.26	4.85752E-09	3.09831E-08	4.00	0.25
3	1.08423E-06	2.10448E-05	2.00	0.42	5.99419E-11	1.14701E-09	4.00	0.57
4	1.20492E-07	7.01640E-06	2.00	1.86	7.39880E-13	4.24756E-11	4.00	1.45
5	1.33883E-08	2.33885E-06	2.00	10.4	9.38138E-15	1.56200E-12	3.98	9.22

TABLE 3. Maximum absolute error of HWCM and HOHWCM solution on scale-3 for $\lambda = 2$ at different resolutions (J) together with the corresponding rate of convergence (ROC) and l_2-norm error (E_{l_2}) for Example 3.1.

J	HWCM-S3				HOHWCM-S3			
	e_J	E_{l_2}	ROC	CPU (in sec.)	e_J	E_{l_2}	ROC	CPU (in sec.)
0	4.25636E-03	3.00372E-03	–	0.10	4.35119E-04	3.07933E-04	–	0.15
1	5.40997E-04	1.10000E-03	1.88	0.12	5.20887E-06	1.07034E-05	4.03	0.12
2	6.09542E-05	3.87441E-04	1.99	0.22	6.38079E-08	3.93424E-07	4.01	0.14
3	6.78310E-06	1.29348E-04	2.00	0.42	7.86990E-10	1.45578E-08	4.00	0.39
4	7.53807E-07	4.31233E-05	2.00	1.68	9.71484E-12	5.39124E-10	4.00	1.51
5	8.37580E-08	1.43747E-05	2.00	11.4	1.20237E-13	1.99658E-11	4.00	9.57

Uncorrected Proof

Example 3.2. *Consider a second Bratu's problem*

$$y'' - \pi^2 e^y = 0, \quad x \in [0, 1], \tag{3.3}$$

$$y(0) = y(1) = 0. \tag{3.4}$$

The closed form solution of Example 3.2 is $y(x) = -\log(1 \pm \cos\pi(x + \frac{1}{2}))$ [34]. It is observed that the solution $y(x) = -\log(1-\cos\pi(x+\frac{1}{2}))$ diverges at $x = \frac{1}{2}$ while the other solution converges and remains bounded. The numerical solution obtained by HOHWCM-S3 is very close to this convergent solution, which can be found via altering $\lambda = -\pi^2$

TABLE 4. Maximum absolute error of HWCM and HOHWCM solution on scale-3 for $\lambda = 3$ at different resolutions (J) together with the corresponding rate of convergence (ROC) and l_2-norm error (E_{l_2}) for Example 3.1.

J	HWCM-S3				HOHWCM-S3			
	e_J	E_{l_2}	ROC	CPU (in sec.)	e_J	E_{l_2}	ROC	CPU (in sec.)
0	2.23174E-02	1.58359E-02	–	0.13	3.63548E-03	2.56784E-03	–	0.12
1	2.86928E-03	5.97149E-03	1.87	0.15	4.50688E-05	8.93419E-05	4.00	0.15
2	3.23914E-04	2.01875E-03	1.99	0.19	5.50172E-07	3.27389E-06	4.01	0.23
3	3.60540E-05	6.73974E-04	2.00	0.41	6.78333E-09	1.21111E-07	4.00	0.38
4	4.00679E-06	2.24697E-04	2.00	1.83	8.37302E-11	4.48486E-09	4.00	1.49
5	4.45208E-07	7.49006E-05	2.00	13.4	1.03362E-12	1.66026E-10	4.00	10.39

TABLE 5. Comparison of absolute error for Example 3.1, taking $\lambda = 1$.

x	HOHWCM-S3			HOHWCM-S2 [38]	LGSM [1]	Decomposition [12]	LTDM [23]	B-Spline [10]	IFD [40]	DTM [18]
	J=4	J=5	J=6							
0.1	$2.32037E-13$	$2.74780E-15$	$3.46945E-17$	$1.29757E-15$	$7.50852E-7$	$2.6851E-3$	$1.9788E-6$	$2.9797E-6$	$1.99412E-10$	-
0.2	4.37608E-13	5.21805E-15	1.38778E-17	3.06699E-15	1.01824E-6	2.0219E-3	3.93944E-6	5.466E-6	3.58880E-10	1.00E-10
0.3	6.00075E-13	7.11930E-15	4.16334E-17	4.17721E-15	9.04748E-7	1.5234E-4	5.8548E-6	7.3357E-6	4.75479E-10	2.00E-10
0.4	7.03909E-13	8.74301E-15	8.32667E-17	2.91434E-15	5.23933E-7	2.2017E-3	7.7038E-6	8.4967E-6	5.46510E-10	2.00E-10
0.5	7.39880E-13	9.02056E-15	2.77556E-17	5.60663E-15	5.06693E-9	3.0155E-3	9.4665E-6	8.8921E-6	5.70298E-10	2.00E-10
0.6	7.03909E-13	8.74301E-15	8.32667E-17	2.91434E-15	5.13861E-7	2.2017E-3	1.11117E-5	8.4967E-6	5.46266E-10	2.00E-10
0.7	6.00089E-13	7.11930E-15	2.77556E-17	4.19109E-15	8.94854E-7	1.5234E-4	1.25716E-5	7.3357E-6	4.75079E-10	3.00E-10
0.8	4.37622E-13	5.27356E-15	1.38778E-17	3.08087E-15	1.00862E-6	2.0219E-3	1.34753E-5	5.466E-6	3.58325E-10	2.00E-10
0.9	2.31669E-13	2.58127E-15	2.77556E-17	1.30451E-15	7.4160E-7	2.6851E-3	1.19678E-5	2.9797E-6	1.98751E-10	2.00E-10

TABLE 6. Comparison of absolute error for Example 3.1, taking $\lambda = 2$.

x	HOHWCM-S3			HOHWCM-S2 [38]	LGSM [1]	LTDM [23]	Decomposition [12]	B-Spline [10]	IFD [40]	DTM [18]
	J=4	J=5	J=6							
0.1	2.58245E-12	3.18495E-14	4.44089E-16	8.96505E-15	4.03416E-6	2.12903E-3	1.52172E-2	1.71789E-5	6.896147E-10	1.30E-6
0.2	5.21994E-12	6.47260E-14	9.15934E-16	2.36200E-14	5.70266E-6	4.2097E-3	1.46751E-2	3.25966E-5	1.27688E-09	2.56E-6
0.3	7.53930E-12	9.31477E-14	1.11022E-15	3.39173E-14	5.22122E-6	6.1868E-3	5.88781E-3	4.48991E-5	1.72268E-09	3.77E-6
0.4	9.14152E-12	1.13076E-13	1.72085E-15	3.11418E-14	3.07485E-6	8.0019E-3	3.24664E-3	5.28584E-5	2.00104E-09	4.87E-6
0.5	9.71484E-12	1.19848E-13	1.38778E-15	4.89608E-14	1.4554E-8	9.5992E-3	6.98508E-3	5.56142E-5	2.09579E-09	5.85E-6
0.6	9.14152E-12	1.13132E-13	1.55431E-15	3.11973E-14	3.04637E-6	1.09295E-2	3.24664E-3	5.28584E-5	2.00186E-09	6.66E-6
0.7	7.53902E-12	9.31477E-14	1.22124E-15	3.38618E-14	5.19455E-6	1.19334E-2	5.88781E-3	4.48991E-5	1.724578E-09	7.29E-6
0.8	5.21996E-12	6.48093E-14	8.32667E-16	2.36755E-14	5.6787E-6	1.23778E-2	1.46751E-2	3.25966E-5	1.27974E-09	7.71E-6
0.9	2.58254E-12	3.19328E-14	3.74700E-16	8.97893E-15	4.01345E-6	1.08734E-2	1.52172E-2	1.71789E-5	6.93327E-10	7.41E-6

Uncorrected Proof

in Eq. (2.37). The absolute errors present in table 7 demonstrate the comparison of HOHWCM-S3 ($J = 6$) with other existing methods, namely HOHWCM-S2 with $J = 9$ [38]; Taylor wavelet (TW) method with resolution level (k) is 1, and degree of polynomial (M) is 11 [22]; and the genetic algorithm (GA), active-set method (ASM) and hybrid GA-ASM [34], the results obtained from these approaches were driven from 100 independent runs.



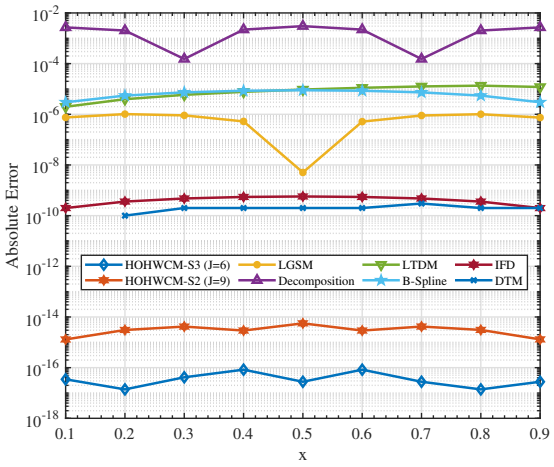


FIGURE 1. Comparison of absolute error of HOHWCM-S3 (J=6) with existing methods for $\lambda = 1$.

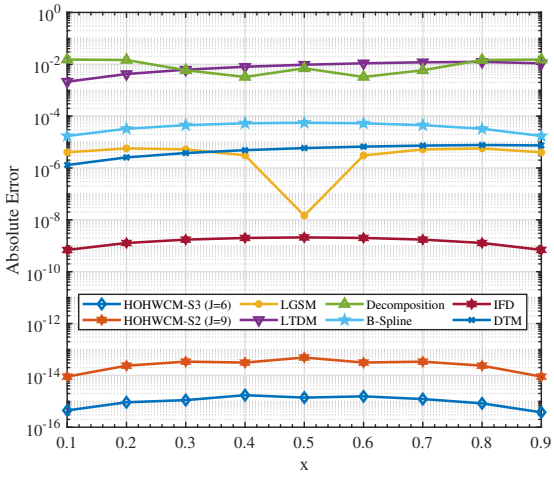


FIGURE 2. Comparison of absolute error of HOHWCM-S3 (J=6) with existing methods for $\lambda = 2$.

TABLE 7. Absolute errors of the Bratu BVP for $\lambda = -\pi^2$.

x	HOHWCM-S3 ($J = 6$)	HOHWCM-S2 ($J = 9$) [38]	TW [22]	GA [34]	ASM [34]	GA-ASM [34]
0.1	$7.4385E{-}15$	$2.16216E{-}13$	$5.5884E{-}8$	$8.2294E{-}3$	$1.4936E{-}6$	$1.6280E{-}7$
0.2	$1.4266E{-}14$	$2.28428E{-}13$	$7.4576E{-}8$	$5.9513E{-}3$	$8.6366E{-}7$	$2.5287E{-}7$
0.3	$1.2768E{-}14$	$2.79110E{-}13$	$1.3357E{-}8$	$4.1528E{-}3$	$9.8907E{-}7$	$3.0937E{-}8$
0.4	$1.4877E{-}14$	$3.33289E{-}13$	$8.9851E{-}8$	$3.0633E{-}3$	$5.1955E{-}7$	$6.8225E{-}7$
0.5	$1.6431E{-}14$	$2.83884E{-}13$	$1.4347E{-}7$	$2.3990E{-}3$	$5.4064E{-}7$	$6.4407E{-}7$
0.6	$1.3545E{-}14$	$3.33067E{-}13$	$8.9851E{-}8$	$1.7599E{-}3$	$5.4935E{-}7$	$1.5643E{-}7$
0.7	$1.2657E{-}14$	$2.79776E{-}13$	$1.3357E{-}8$	$9.4572E{-}4$	$2.4552E{-}7$	$7.0467E{-}7$
0.8	$1.4710E{-}14$	$2.29539E{-}13$	$7.4576E{-}8$	$6.3272E{-}5$	$3.3472E{-}7$	$9.7341E{-}7$
0.9	$7.9381E{-}15$	$2.16605E{-}13$	$5.5884E{-}8$	$7.6186E{-}4$	$2.6137E{-}7$	$1.2930E{-}6$

Uncorrected Proof

Example 3.3. *Consider a third Bratu's problem*

$$y'' + \pi^2 e^{-y} = 0, \quad x \in [0, 1], \tag{3.5}$$

$$y(0) = y(1) = 0. \tag{3.6}$$

The most precise form of two exact solution for Example 3.3 studied in literature [13, 34] is $y(x) = \log(1 \pm \sin(\pi x))$. However, the numerical outcomes driven from the present technique shows the better agreement with $y(x) = \log(1 + \sin(\pi x))$, which can be found via altering $\lambda = \pi^2$ in Eq. (2.37). The comparison of absolute errors of HOHWCM-S3 ($J = 6$) with the genetic algorithm (GA), active-set method (ASM) and hybrid GA-ASM [34] has been shown in Table 8.

TABLE 8. Absolute errors of the Bratu BVP for $\lambda = \pi^2$.

x	HOHWCM-S3 ($J = 6$)	GA [34]	ASM [34]	GA-ASM [34]
0.1	$7.4385E{-}15$	$4.32230E{-}3$	$1.60860E{-}6$	$3.44860E{-}5$
0.2	$1.4433E{-}14$	$1.10170E{-}3$	$6.29960E{-}6$	$2.47300E{-}5$
0.3	$1.2768E{-}14$	$1.60570E{-}3$	$5.73070E{-}6$	$1.86290E{-}5$
0.4	$1.4877E{-}14$	$3.51920E{-}3$	$2.32950E{-}6$	$1.24610E{-}5$
0.5	$1.6431E{-}14$	$5.47830E{-}3$	$8.03400E{-}6$	$1.63980E{-}5$
0.6	$1.3545E{-}14$	$8.33590E{-}3$	$4.19330E{-}7$	$1.11440E{-}5$
0.7	$1.2657E{-}14$	$1.20770E{-}2$	$7.39800E{-}6$	$4.45450E{-}6$
0.8	$1.4710E{-}14$	$1.61510E{-}2$	$4.13610E{-}6$	$7.70660E{-}6$
0.9	$7.9381E{-}15$	$2.08810E{-}2$	$2.62840E{-}6$	$4.45110E{-}6$

4. CONCLUSION

An efficient numerical techniques based on non-dyadic (scale-3) Haar wavelet (HWCM-S3) and its advancement (HOHWCM-S3) have been established and employed on highly non-linear Bratu's problem. To show the effectiveness and accuracy of the proposed methods, different variants of Bratu's problems have been tested and compared with existing methods. Some findings based on the tested problems are discussed as follows:

- The accuracy and efficiency of the HOHWCM-S3 examined using maximum absolute error, l_2 norm error, as shown in Tables 1 to 4. The result obtained from the HOHWCM-S3 compared with the other existing methods such as LGSM [1], DTM [18], LTDM [23], B-spline [10], IFD [40], Decomposition [12]; as shown in Tables 5 and 6. HOHWCM-S3 gives more accurate results than all of these methods.
- The performance of the HOHWCM-S3, computed at resolution $J = 6$, also compare with the spline-based and wavelet-based methods; the comparison is presented in Table 9. Among the spline-based methods, the cubic BSM [2] uses $n = 10$ for $\lambda = 1$; optimal BSM [2] uses $n = 160$ mesh points for $\lambda = 1$ and $\lambda = 2$; and QBSM [35] uses $n = 256$ mesh points for both $\lambda = 1$ and $\lambda = 2$. Among the wavelet-based methods, the Taylor wavelet (TW) method [22] with resolution (k) is 1 and degree of polynomial (M) is 10; the Mexican hat wavelet (MHW) method [28] using 10 neurons and 30 weights, 100 independent runs for $\lambda = 1$ and $\lambda = 2$; and the Chebyshev wavelet (CW) method [44] with $k = 2$ and $M = 8$ for $\lambda = 2$. For both values of λ, these existing methods are applied on a fixed mesh or at a fixed resolution, so their accuracy is depend on that choice. HOHWCM-S3 is multiresolution in nature, and their accuracy is achieved by increasing the resolution level (J).

TABLE 9. Comparison of maximum absolute error for different methods.

λ	HOHWCM-S3 ($J = 6$)	Spline-based method			Wavelet-based method		
		Cubic BSM [2]	Optimal BSM [2]	QBSM [35]	TW [22]	MHW [28]	CW [44]
1	$3.88578E-16$	–	$1.81E{-}7$	$6.41E{-}13$	$7.76E{-}12$	$1.90E{-}8$	–
2	$1.94289E-15$	$3.48E{-}6$	$3.94E{-}11$	$9.01E{-}12$	$1.19E{-}9$	$3.75E{-}8$	$7.18825E{-}6$

- Tables 7 and 8 give the comparison of the results obtained by HOHWCM-S3 with various existing techniques, namely HOHWCM-S2 [38] with $J = 9$; TW method [22] with ($k = 1, M = 11$); and the GA, ASM and GA-ASM [34], these approaches are based on neural network and all finding obtained by using 100 independent runs.

Uncorrected Proof

ACKNOWLEDGMENT

The authors express their gratitude to the anonymous reviewers for their insightful suggestions and comments.

References

[1] S. Abbasbandy, M. Hashemi, and C. S. Liu, *The Lie-group shooting method for solving the Bratu's equation*, Communications in Nonlinear Science and Numerical Simulation, *16*(11) (2011), 4238–4249.

[2] M. Abukhaled, S. Khuri, and A. Sayfy, *Spline-based numerical treatments of Bratu-type equations*, Palestine J. Math, *1* (2012), 63–70.

[3] A. Adewumi, A. Aderogba, S. Akindeinde, O. Fabelurin, and R. Lebelo, *Finite difference spectral collocation schemes for the solutions of boundary value problems*, Heliyon, *10*(1) (2024).

[4] R. Amin, K. Shah, Q. M. Al-Mdallal, I. Khan, and M. Asif, *Efficient numerical algorithm for the solution of eight order boundary value problems by Haar wavelet method*, International Journal of Applied and Computational Mathematics, *7* (2021), 1–18.

[5] S. Arora and R. Kumar, *Application of Haar-scale-3 wavelet collocation method to the solution of Fitzhugh–Nagumo non-linear partial differential equation*, Research in Mathematics, *12*(1) (2025), 2463183.

[6] U. M. Ascher, R. M. Mattheij, and R. D. Russell, *Numerical solution of boundary value problems for ordinary differential equations*, SIAM, 1995.

[7] M. Baccouch and H. Temimi, *A new derivation of the closed-form solution of Bratu's problem*, International Journal of Applied and Computational Mathematics, *9*(5) (2023),100.

[8] E. Bachini, V. Krause, and A. Voigt, *The interplay of geometry and coarsening in multicomponent lipid vesicles under the influence of hydrodynamics*, Physics of Fluids, *35*(4) (2023), 042102.

[9] J. P. Boyd, *One-point pseudospectral collocation for the one-dimensional Bratu equation*, Applied Mathematics and Computation, *217*(12) (2011), 5553–5565.

[10] H. Caglar, N. Caglar, M. Özer, A. Valarıstos, and A. N. Anagnostopoulos, *B-spline method for solving Bratu's problem*, International Journal of Computer Mathematics, *87*(8) (2010), 1885–1891.

[11] C. K. Chui and J. ao Lian, *Construction of compactly supported symmetric and antisymmetric orthonormal wavelets with scale = 3*, Applied and Computational Harmonic Analysis, *2*(1) (1995), 21–51.

[12] E. Deeba, S. Khuri, and S. Xie, *An algorithm for solving boundary value problems*, Journal of Computational Physics, *159*(2) (2000), 125–138.

[13] S. Deniz and N. Bildik. *Optimal perturbation iteration method for Bratu-type problems*, Journal of King Saud University-Science, *30*(1) (2018), 91–99.

[14] M. A. El-Hady, M. El-Gamel, M. Izadi, and A. El-shenawy, *Numerical computation of nonlinear boundary value problems in heat transfer and chemical engineering: a robust Lucas–Fibonacci series approach*, Journal of Taibah University for Science, *19*(1) (2025), 2477917.

[15] D. A. Frank-Kamenetskii, *Towards temperature distributions in a reaction vessel and the stationary theory of thermal explosion*, In *Doklady Acad. Nauk SSSR*, volume 18, 1938.

[16] D. A. Frank-Kamenetskii, *Diffusion and heat exchange in chemical kinetics*, Princeton University Press, 2015.

[17] I. M. Gelfand, *Some problems in the theory of quasilinear equations*, Uspekhi Mat. Nauk, *14* (1959), 87–158.

[18] I. Hassan and V. S. Ertürk, *Applying differential transformation method to the one-dimensional planar Bratu problem*, Int. J. Contemp. Math. Sciences, *2*(30) (2007), 1493–1504.

[19] M. Izadi and H. M. Srivastava, *Generalized bessel quasilinearization technique applied to Bratu and Lane–Emden-type equations of arbitrary order*, Fractal and Fractional, *5*(4) (2021), 179.

[20] J. Jacobsen and K. Schmitt, *The Liouville–Bratu–Gelfand problem for radial operators*, Journal of Differential Equations, *184*(1) (2002), 283–298.

[21] H. Kaur, R. Mittal, and V. Mishra, *Haar wavelet approximate solutions for the generalized Lane–Emden equations arising in astrophysics*, Computer Physics Communications, *184*(9) (2013), 2169–2177.

[22] E. Keshavarz, Y. Ordokhani, and M. Razzaghi. *The Taylor wavelets method for solving the initial and boundary value problems of Bratu-type equations*, Applied Numerical Mathematics, *128* (2018), 205–216.

[23] S. A. Khuri, *A new approach to Bratu's problem*, Applied mathematics and computation, *147*(1) (2004), 131–136.

[24] L. Kivistik, M. Mehrparvar, M. Eerme, and J. Majak, *Dynamics of flight of the fragments with higher order Haar wavelet method*, Proceedings of the Estonian Academy of Sciences, *73*(2) (2024).

Uncorrected Proof

[25] N. Kumar, L. N. Kannaujiya, and A. K. Verma, *Uniform Haar wavelet solutions for fractional regular α-singular bvps modeling human head heat conduction under Febrifuge effects*, Mathematical Methods in the Applied Sciences, *48*(8) (2025), 8568–8582.

[26] J. Majak, M. Pohlak, M. Eerme, and B. Shvartsman, *Solving ordinary differential equations with higher order Haar wavelet method* In *AIP Conference Proceedings*, AIP Publishing LLC, *2116* (2019), page 330002.

[27] J. Majak, M. Pohlak, K. Karjust, M. Eerme, J. Kurnitski, and B. Shvartsman, *New higher order Haar wavelet method: Application to FGM structures*, Composite Structures, *201* (2018), 72–78.

[28] Z. Masood, K. Majeed, R. Samar, and M. A. Z. Raja, *Design of Mexican Hat wavelet neural networks for solving Bratu type nonlinear systems*, Neurocomputing, *221* (2017), 1–14.

[29] R. Mittal and S. Pandit, *Quasilinearized scale-3 Haar wavelets-based algorithm for numerical simulation of fractional dynamical systems*, Engineering Computations, *35*(5) (2018), 1907–1931.

[30] R. C. Mittal and S. Pandit, *New scale-3 Haar wavelets algorithm for numerical simulation of second order ordinary differential equations*, Proceedings of the National Academy of Sciences, India Section A: Physical Sciences, *88*(4) (2018).

[31] H. Mohammadi, H. Saeedi, and M. Izadi, *A novel projection method utilizing Krawtchouk wavelets for solving fractional-order optimal control models*, International Journal of Dynamics and Control, *13*(9) (2025), 297.

[32] S. Pandit, *Local radial basis functions and scale-3 Haar wavelets operational matrices based numerical algorithms for generalized regularized long wave model*, Wave Motion, *109* (2022), 102846.

[33] M. P. Preetham and S. Kumbinarasaiah, *A numerical study of two-phase nanofluid mhd boundary layer flow with heat absorption or generation and chemical reaction over an exponentially stretching sheet by Haar wavelet method*, Numerical Heat Transfer, Part B: Fundamentals, *85*(6) (2024), 706–735.

[34] M. A. Z. Raja, R. Samar, E. S. Alaidarous, and E. Shivanian, *Bio-inspired computing platform for reliable solution of Bratu-type equations arising in the modeling of electrically conducting solids*, Applied Mathematical Modelling, *40*(11-12) (2016), 5964–5977.

[35] P. Roul and K. Thula, *A fourth-order B-spline collocation method and its error analysis for Bratu-type and Lane–Emden problems*, International Journal of Computer Mathematics, *96*(1) (2019),85–104.

[36] A. R. Shouman, *A review of one aspect of the thermal-explosion theory*, Journal of engineering mathematics, *56*(2) (2006), 179–184.

[37] R. Singh, J. Shahni, H. Garg, and A. Garg, *Haar wavelet collocation approach for Lane-Emden equations arising in mathematical physics and astrophysics*, The European Physical Journal Plus, *134*(11) (2019), 548.

[38] Swati, M. Singh, and K. Singh, *An advancement approach of Haar wavelet method and Bratu-type equations*, Applied Numerical Mathematics, *170* (2021), 74–82.

[39] Swati, M. Singh, and K. Singh, *An efficient technique based on higher order Haar wavelet method for Lane–Emden equations*, Mathematics and Computers in Simulation, *206* (2023), 21–39.

[40] H. Temimi and M. Ben-Romdhane, *An iterative finite difference method for solving Bratu's problem*, Journal of Computational and Applied Mathematics, *292* (2016), 76–82.

[41] A. K. Verma and D. Tiwari, *Higher resolution methods based on quasilinearization and Haar wavelets on Lane–Emden equations*, International Journal of Wavelets, Multiresolution and Information Processing, *17*(03) (2019), 1950005.

[42] A. M. Wazwaz, *Adomian decomposition method for a reliable treatment of the Bratu-type equations*, Applied Mathematics and Computation, *166*(3) (2005), 652–663.

[43] P. Yadav, S. Jahan, and M. Izadi, *Taylor wavelet quasilinearization method for solving tumor growth model of fractional order*, Results in Control and Optimization, *15* (2024), 100437.

[44] C. Yang and J. Hou, *Chebyshev wavelets method for solving Bratu's problem*, Boundary value problems, *2013*(1) (2013), 142.

Uncorrected Proof